Earth Syst. Dynam. Discuss., https://doi.org/10.5194/esd-2018-34
Manuscript under review for journal Earth Syst. Dynam.
Discussion started: 7 June 2018

Earth System Dynamics
Discussions
Open Access
EGU

A theoretical approach to assess soil moisture–climate coupling across CMIP5 and GLACE-CMIP5 experiments

Clemens Schwingshackl[1], Martin Hirschi[1], and Sonia I. Seneviratne[1]

[1]Institute for Atmospheric and Climate Science, ETH Zürich, Universitätsstrasse 16, 8092 Zürich, Switzerland

Correspondence to: Clemens Schwingshackl (clemens.schwingshackl@env.ethz.ch)

Abstract. Terrestrial climate is influenced by various land–atmosphere interactions that involve numerous land surface state variables. In several regions on Earth, soil moisture plays an important role for climate through its control on the partitioning of net radiation into sensible and latent heat fluxes and, consequently, its impact on temperature and precipitation. The Global Land-Atmosphere Climate Experiment–Coupled Model Intercomparison Project phase 5 (GLACE-CMIP5) aims to quantify the impact of soil moisture on these important climate variables and to trace the individual coupling mechanisms. GLACE-CMIP5 provides experiments with different soil moisture prescriptions that can be used to isolate the effect of soil moisture on climate. Using a theoretical approach that relies on the distinct relation of soil moisture with evaporative fraction (the ratio of latent heat flux over net radiation) and daily maximum near-surface air temperature in different soil moisture regimes, the climate impact of the soil moisture prescriptions in the GLACE-CMIP5 experiments can be emulated and quantified. The theoretical estimation of the soil moisture effect on evaporative fraction agrees very well with estimations obtained directly from the GLACE-CMIP5 experiments (pattern correlation of 0.85). Moreover, the soil moisture effect on daily maximum temperature is well captured in those regions where soil moisture exerts a strong control on latent heat fluxes. The theoretical approach is further applied to quantify the soil moisture contribution to the projected change of the temperature on the hottest day of the year, confirming recent estimations by other studies. Finally, GLACE-style soil moisture prescriptions are emulated in an extended set of CMIP5 models. The results indicate consistency between the soil moisture–climate coupling strength estimated with GLACE-CMIP5 and CMIP5 models. Although the theoretical approach is designed to capture only the local soil moisture–climate coupling strength, it can also help to distinguish non-local from local soil moisture–atmosphere feedbacks where sensitivity experiments (such as GLACE-CMIP5) are available. Overall, the presented theoretical approach constitutes a simple and powerful tool to quantify local soil moisture–climate coupling in both GLACE-CMIP5 and CMIP5 models that can be applied in the absence of dedicated sensitivity experiments.

1 Introduction

The amount of available energy at the surface is a key driver for climate on Earth. It provides the first-order control for the location of the different climate zones and is an important contributor to weather and climate variations at daily, seasonal, and longer-term timescales. Absorbed shortwave and net longwave radiation at the surface constitute the inputs for the available energy, the so called net radiation. This energy is used for evaporation and transpiration of water from soils and plants, it is

Earth Syst. Dynam. Discuss., https://doi.org/10.5194/esd-2018-34
Manuscript under review for journal Earth Syst. Dynam.
Discussion started: 7 June 2018

transported as heat to the atmosphere, and it warms up the soil. The partitioning of net radiation into these latent, sensible, and ground heat fluxes is of fundamental importance for the investigation of climate because the shares of the single fluxes influence various basic climate variables, such as temperature, precipitation, and atmospheric humidity.

In several regions of the world, soil moisture impacts the partitioning of net radiation by exerting control on latent heat flux (Koster et al., 2004; Seneviratne et al., 2010). Numerous studies analyzed the coupling strength between soil moisture and latent heat flux and tried to identify the regions where soil moisture influences atmospheric conditions and, thus, climate. Using the correlation between evapotranspiration and radiation and contrasting it to the correlation between evapotranspiration and precipitation, Teuling et al. (2009) identified regions with either radiation or soil moisture control on latent heat flux. Dirmeyer (2011) introduced a metric that combines the sensitivity of latent heat flux to soil moisture changes with typical soil moisture variations and quantified the coupling strength therewith. Koster et al. (2009) used an idealized framework for describing the relation between soil moisture and evaporative fraction (the share of net radiation going into latent heat flux) that allows to distinguish between different soil moisture regimes (Koster et al., 2009; Seneviratne et al., 2010).

Other metrics focus on the impact of soil moisture changes on atmospheric variables. Koster et al. (2004) used the precipitation based Ω_P-metric (introduced by Koster et al., 2000) to quantify the impact of soil moisture on precipitation. Adapting this measure to investigate the effect of soil moisture on temperature, Seneviratne et al. (2006) showed the importance of land–atmosphere coupling for future summer temperature projections in Europe. Soil moisture–temperature coupling was further examined by Miralles et al. (2012) who established the Π-metric, which is based on the correlation of (potential) sensible heat flux and temperature. They used it to identify regions with strong soil moisture effects on temperature. Zscheischler et al. (2015) introduced the Vegetation–Atmosphere Coupling (VAC) index that can serve as proxy for estimating the coupling strength between soil moisture and latent heat flux. This index was used by Sippel et al. (2017) to diagnose land–atmosphere coupling in climate models, reanalyses, and observation based datasets. Their results indicate an overestimation of land–atmosphere coupling in models participating in the Coupled Model Intercomparison Project phase 5 (CMIP5). Other approaches to diagnose land–atmosphere interactions include wavelet correlation analysis (Casagrande et al., 2015) or consider processes in the atmospheric boundary layer to reflect the full land–atmosphere coupling chain (Santanello et al., 2011; Miralles et al., 2014; Santanello et al., 2015).

Through its control on the partitioning of net radiation into latent and sensible heat fluxes, soil moisture can have a pronounced impact on near-surface air temperature (Seneviratne et al., 2010; Miralles et al., 2012; Hirschi et al., 2014; Schwingshackl et al., 2017). Particulary during droughts and heat waves the impact of soil moisture on temperature can become very strong. Using the standardized precipitation index (SPI) as a proxy for soil moisture, Hirschi et al. (2011) and Mueller and Seneviratne (2012) showed that in transitional climate regimes the number of heat wave days in the hottest month of the year depends on preceding moisture conditions. Moreover, soil moisture and the yearly maximum value of daily maximum temperature TX_x exhibit a negative linear relationship in Europe (Whan et al., 2015), emphasizing the crucial role of soil moisture for temperature extremes. Miralles et al. (2014) highlighted the importance of both soil moisture–temperature coupling and boundary layer feedbacks for the evolution of the 2003 European heat wave and the 2010 heat wave in Russia. Performing

Earth Syst. Dynam. Discuss., https://doi.org/10.5194/esd-2018-34
Manuscript under review for journal Earth Syst. Dynam.
Discussion started: 7 June 2018

modeling experiments, Hauser et al. (2016) showed that extreme soil moisture conditions as observed during the 2010 Russian heat wave strongly contribute to increased risks of similar events.

Studying soil moisture–climate coupling is often limited by the sparse availability of soil moisture observations. In situ measurements are relatively rare and restricted to a few regions (Seneviratne et al., 2010; Dorigo et al., 2011). For global studies, an alternative approach consists in using satellite-based soil moisture estimates. While satellites provide quasi-global coverage, data availability is poor in regions with dense vegetation cover and reliable soil moisture measurements are only available since the 1990s (de Jeu et al., 2008; Dorigo et al., 2017). Moreover, remote-sensing can only provide surface soil moisture but no direct root zone soil moisture estimations.

As a consequence of these limitations for the use of observations, model simulations have been widely employed to investigate the impact of soil moisture on atmospheric conditions and climate. The Global Land-Atmosphere Climate Experiments (GLACE-1 and GLACE-2; Koster et al., 2006, 2010; van den Hurk et al., 2011), for example, were used to investigate soil moisture–precipitation and soil moisture–temperature coupling on seasonal timescales. For studying long-term effects, these experiments were further extended to include several CMIP5 models (GLACE-CMIP5; Seneviratne et al., 2013). GLACE-CMIP5 was extensively used to investigate various features of land–atmosphere coupling. Berg et al. (2014) analyzed soil moisture–atmosphere interactions, in particular their effect on temperature, in GFDL Earth System Model simulations that contributed to GLACE-CMIP5. Lorenz et al. (2015) performed GLACE-1 and GLACE-CMIP5 experiments with the ACCESS1.3b model and applied several land–atmosphere coupling measures to investigate the impact of soil moisture on atmospheric conditions in the different soil moisture experiments. Berg et al. (2015) investigated terrestrial and atmospheric contributions to the correlation between temperature and precipitation using the GLACE-CMIP5 experiments. Moreover, soil moisture trends and land–atmosphere feedbacks were found to contribute to future aridity increase (Berg et al., 2016) and to be important for explaining future temperature and precipitation changes in the tropics (May et al., 2015).

Additionally, GLACE-CMIP5 models were used to study the impact of soil moisture on extremes. Lorenz et al. (2016) highlighted the effect of soil moisture on both temperature and precipitation extremes. However, they also found that the large variability of soil moisture trends in the single GLACE-CMIP5 models leads to large uncertainties for projections of future climate extremes. Recently, Vogel et al. (2017) showed that the soil moisture prescription in the different GLACE-CMIP5 experiments has a strong impact on TX_x with higher TX_x occurring at lower soil moisture contents.

GLACE-CMIP5 simulations provide thus a rich source to examine soil moisture–climate coupling. Moreover, the fact that the single simulations only differ from each other in the way soil moisture is prescribed, makes it possible to attribute emerging differences to the soil moisture shifts. Here we present a theoretical approach to quantify the effect that the different soil moisture prescriptions in the various GLACE-CMIP5 experiments have on evaporative faction EF and daily maximum near-surface air temperature TX. The approach is based on the distinct impact of soil moisture θ on EF and TX in different soil moisture regimes. A major advantage of this theoretic approach is that it enables to emulate GLACE-style soil moisture prescription. In particular, it can be applied directly to CMIP5 models without the need of performing additional model simulations. We use this approach to investigate how soil moisture shifts across GLACE-CMIP5 experiments influence EF and TX. Additionally,

Earth Syst. Dynam. Discuss., https://doi.org/10.5194/esd-2018-34
Manuscript under review for journal Earth Syst. Dynam.
Discussion started: 7 June 2018

the resulting relations are applied to estimate the soil moisture contribution to TX_x and compared to the Vogel et al. (2017) estimations.

2 Theoretical background: $EF(\theta)$ framework

Soil moisture can have an impact on the exchange of water and energy between land and atmosphere through its control on latent heat flux. This relationship can be specified using a simple framework that connects EF to soil moisture (Koster et al., 2009; Seneviratne et al., 2010). The framework, illustrated in Figure 1a, distinguishes between three different soil moisture regimes: 1) the wet soil moisture regime where EF is independent of soil moisture, 2) the transitional regime in which EF and soil moisture are linearly coupled, and 3) the dry regime in which EF is zero. Schwingshackl et al. (2017) show the applicability of this framework to describe spatio-temporal variations of the $EF(\theta)$ relationship for several datasets and use the resulting $EF(\theta)$ curve to classify the different soil moisture regimes. They further employ the framework to analyze the effect of soil moisture variations on the surface energy balance and TX individually in the different regimes.

Based on ten-fold cross validation their methodology first selects for each grid point separately the best curve for describing $EF(\theta)$ from a pool of possible, preselected functions. The obtained functional relationship is then used to estimate the two soil moisture values that separate the three regimes, that is, the wilting point (θ_{wilt}), separating dry and transitional regimes, and the critical point (θ_{crit}), separating the transitional and wet regimes. This allows for the unique attribution of each daily soil moisture value to one soil moisture regime and to analyze the effect of soil moisture variations on atmospheric conditions in each regime individually.

Using this approach, the sensitivity of EF to soil moisture variations (i.e., the gradient $\partial EF/\partial\theta$) can be estimated in the different soil moisture regimes separately. (Note that although the $EF(\theta)$ framework requires a constant line in the wet regime, the actual fitting routine optimizes the location of the wilting and critical points. As a result, when calculating $\partial EF/\partial\theta$ from the daily EF and soil moisture estimates, the slope in the wet regime is small, but not necessarily identical to zero.) Similarly, the sensitivity of TX to soil moisture changes can be quantified in each regime. The sensitivity is expected to differ between the soil moisture regimes due to the distinct impact of soil moisture on the partitioning of net radiation into latent and sensible heat fluxes in each of the regimes. The gradient $\partial TX/\partial\theta$ is strongest in the transitional regime, in which soil moisture has an impact on EF, while in the dry and wet regimes the impact of soil moisture on TX is small (Schwingshackl et al., 2017). Whenever the soil moisture content crosses the regime borders, the soil moisture effect on EF and TX is a mixture of the sensitivities in the different soil moisture regimes.

Schwingshackl et al. (2017) provide a theoretical approach that can easily be applied to quantify the effect of soil moisture variations on EF and TX based on the distinct sensitivities in the different soil moisture regimes. In the following, this approach is applied to investigate soil moisture–climate coupling in CMIP5 and in the GLACE-CMIP5 experiments.

Earth Syst. Dynam. Discuss., https://doi.org/10.5194/esd-2018-34
Manuscript under review for journal Earth Syst. Dynam.
Discussion started: 7 June 2018

3 Methods and Data

3.1 Data

3.1.1 GLACE-CMIP5

Direct estimations of the coupling strength between different Earth system variables are often challenging due to the system's complex feedback structures. One option to tackle this issue is to employ idealized climate modeling experiments. GLACE-CMIP5 (Seneviratne et al., 2013) tackles the question to which extent soil moisture influences climate due to its impact on land–atmosphere coupling. GLACE-CMIP5, for which six CMIP5 modeling groups contributed the necessary model runs, includes three soil moisture experiments: 1) a control run (*CTL*) with interactive soil moisture and prescribed sea surface temperatures, sea ice, land use, and atmospheric CO_2 concentrations from the respective CMIP5 historical and Representative Concentration Pathway 8.5 (RCP8.5; Riahi et al., 2011) simulation, 2) a model run with prescribed soil moisture as 1971–2000 climatology of the control run ("EXP A", here referred to as *Clim20C*), and 3) a model run with soil moisture prescribed as transient climatology of the control run ("EXP B", here referred to as *ClimCTL*). An example of the soil moisture evolution in the different experiments is shown in Figure 1b for *CTL* and *Clim20C* and in supplementary Figure S1 for *CTL* and *ClimCTL*. While *ClimCTL* is aimed to eliminate the (short-term) interannual soil moisture variability, in *Clim20C* additionally long-term soil moisture trends are removed.

Four out of the six available GLACE-CMIP5 models provide all necessary daily data for the analysis performed in this study. These are ACCESS, EC-EARTH, GFDL's ESM2M, and MPI-ESM-LR (see supplementary Table S1). The soil moisture prescription in ACCESS *Clim20C* has a known issue, namely a shift of the seasonal cycle between 2039/40 and 2089/90 (R. Lorenz, ETH Zürich, 2017, personal communication). As we rely on own re-computed soil moisture climatologies (see Figure 1b and supplementary Figure S1) for the theoretical approach, this shift should, however, not affect the estimated effects.

3.1.2 CMIP5

Additionally to the GLACE-CMIP5 runs, the output of 20 CMIP5 models (Taylor et al., 2012) from historical simulations and the RCP8.5 scenario is used. The models are selected based on the availability of the daily data that are necessary for performing the analysis. A list with all used CMIP5 models can be found in supplementary Table S1.

While the analysis presented here uses total column soil moisture, the CMIP5 model standard output only provides daily data for soil moisture in the top soil layer. For total column soil moisture only monthly data are available. Daily total column soil moisture θ is thus reconstructed using the water balance equation:

$$\theta(t+1) = \theta(t) + P(t) - \mathrm{ET}(t) - R(t) - \Delta h_{\mathrm{snow}} \tag{1}$$

where P is precipitation, ET is evapotranspiration, R is total runoff, and Δh_{snow} is the change of surface snow (in water equivalent) between time steps (days) t and $t+1$. The starting value $\theta(t=0)$ can be chosen arbitrarily as for the analysis applied here only soil moisture variability and trends are relevant. The reconstructed time series spans the period 1950 to 2100.

Earth Syst. Dynam. Discuss., https://doi.org/10.5194/esd-2018-34
Manuscript under review for journal Earth Syst. Dynam.
Discussion started: 7 June 2018

Note that we do not consider the canopy reservoir as it is usually small. However, in regions with dense vegetation and shallow soils it might introduce some uncertainty in Eq. (1).

To remove any artificial drifts imposed by Eq. (1), the reconstructed daily total column soil moisture estimates are linearly detrended on each grid box individually. Additionally, the multi-year variability of the reconstructed time series is adjusted to match the variability of the monthly soil moisture data that are available in the CMIP5 archive: First, we subtract the three-year running mean from the reconstructed daily data and, then, we add back the three-year running mean of the monthly CMIP5 soil moisture values (which are interpolated to daily values by cubic spline) to the reconstructed soil moisture series. To reassure that these corrected daily soil moisture values are in agreement with the CMIP5 soil moisture, monthly means of the corrected daily soil moisture values are compared to the CMIP5 monthly soil moisture content. We require that the correlation between both estimates over the whole period 1950 to 2100 is higher than 0.99 and that the root mean squared error is smaller than 10 % of the standard deviation of the monthly CMIP5 soil moisture. Grid points on which these criteria are not met are not considered in the analysis in the respective model. A map with the final number of CMIP5 models considered at each grid cell is shown in supplementary Figure S2.

3.1.3 Data preparation

Soil moisture effects on climate are examined with two different measures. The *experiment-based* effect is obtained directly from the GLACE-CMIP5 experiments, while the *sensitivity-based* effect is based on theoretical calculations of soil moisture–climate coupling and can thus be applied to both GLACE-CMIP5 and CMIP5 to emulate *Clim20C* and *ClimCTL* (see Sections 3.2 and 3.3 for more details about the derivation of the measures).

For each model of GLACE-CMIP5 and CMIP5, the methodology of Schwingshackl et al. (2017) is applied to identify the different soil moisture regimes, which are required to calculate the sensitivity-based effect. The $\mathrm{EF}(\theta)$ relationships and the soil moisture regime classifications (see Section 2) are obtained with data of the control run only. Daily data for total column soil moisture (calculated with Eq. (1) for the CMIP5 models), latent heat flux, sensible heat flux, net radiation, and daily maximum near-surface air temperature are used. Following the procedure of Berg et al. (2017), soil moisture data are normalized by the standard deviation of all daily soil moisture values of the control run in the reference period 1970–1999 on each grid point separately for each model individually before performing the analysis. Following the methodology of Schwingshackl et al. (2017), the experiment- and sensitivity-based effects (see Sections 3.2 and 3.3) are estimated for twelve different 3-month subsets individually (i.e., all data from January–March, February–April,... December–February in the respective time period are pooled separately) and then averaged. The number of 3-month subsets on a grid point might be less than twelve since we require that all involved variables for calculating EF are positive (see Schwingshackl et al. (2017) for details).

By calculating the sensitivity-based effect, GLACE-style soil moisture prescriptions can be theoretically emulated with CMIP5 models (see Sections 3.2 and 3.3). For this purpose, soil moisture values equivalent to the ones in *Clim20C* and *ClimCTL* of GLACE-CMIP5 (see Figure 1b and supplementary Figure S1) are calculated for all CMIP5 models using the reconstructed daily total column soil moisture estimates and following the procedure for calculating prescribed soil moisture in the different GLACE-CMIP5 experiments (Seneviratne et al., 2013). Similarly, $\theta_{\mathrm{Clim20C}}$ and $\theta_{\mathrm{ClimCTL}}$ is also calculated for

Earth Syst. Dynam. Discuss., https://doi.org/10.5194/esd-2018-34
Manuscript under review for journal Earth Syst. Dynam.
Discussion started: 7 June 2018

the GLACE-CMIP5 models. By combining these soil moisture estimates with the distinct sensitivities of EF to soil moisture in the single soil moisture regimes the sensitivity-based effect can be estimated (see Section 3.2).

The analysis is performed for the time span 2070–2099 on each grid point individually. Additionally, for investigating the effect of soil moisture on the yearly maximum value of daily maximum temperature TX_x five different time periods are used depending on the model-dependent year when global mean temperature increase ΔT_{glob} reaches 1.0 K, 1.5 K, 2.0 K, 2.5 K, and 3.0 K above preindustrial temperature levels. To be consistent with the GLACE-CMIP5 simulations, which only start in 1951, 1951–1970 is chosen as reference period for ΔT_{glob} and 0.22 K is added to account for the T_{glob} increase that happened between 1871–1890 and 1951–1970 according to the 20 CMIP5 models used in this study. ΔT_{glob} is smoothed with a 20-year window to eliminate short-term variations in order to uniquely identify the year in which ΔT_{glob} reaches 1.0 K, 1.5 K, 2.0 K, 2.5 K, and 3.0 K. The analysis is then performed considering data from a 20 year window centered around the selected year. TX_x changes (i.e., ΔTX_x) are as well based on the reference period 1951–1970 (calculated on each grid point individually and for GLACE-CMIP5 in each experiment separately). To be consistent with the methodology for T_{glob} and to start from the same level, an offset of 0.22 K is added as well.

The effect of soil moisture prescription on TX_x is analyzed for a couple of regions that are known to have strong soil moisture–climate coupling. The considered regions correspond to the ones defined in the Special Report on Managing the Risks of Extreme Events and Disasters to Advance Climate Change Adaptation (SREX; Seneviratne et al., 2012).

3.2 Estimating the soil moisture effect on evaporative fraction

For the GLACE-CMIP5 models, the output of the three experiments *CTL*, *Clim20C*, and *ClimCTL* can be used to directly estimate the *experiment-based* effect of the different soil moisture prescriptions on EF. For this purpose, daily differences of soil moisture $\Delta\theta$ and evaporative fraction ΔEF are calculated across experiments and the average effect of soil moisture shifts on EF (i.e., $\Delta\mathrm{EF}/\Delta\theta$) is quantified from the slope of a linear fit between $\Delta\theta$ and ΔEF (without allowing for a constant term).

Additionally, $\Delta\mathrm{EF}/\Delta\theta$ estimates can be reproduced considering the three different soil moisture regimes according to the $\mathrm{EF}(\theta)$ framework and the distinct sensitivities $\partial\mathrm{EF}/\partial\theta$ within them (Figure 1a). When soil moisture changes across regime limits, the average effect on EF can be assumed to be a mixing of the sensitivities in the respective regimes:

$$\frac{\Delta\mathrm{EF}}{\Delta\theta} = \frac{\theta_{\mathrm{start}} - \theta_{\mathrm{crit}}}{\theta_{\mathrm{start}} - \theta_{\mathrm{end}}} \left.\frac{\partial\mathrm{EF}}{\partial\theta}\right|_{\mathrm{wet}} + \frac{\theta_{\mathrm{crit}} - \theta_{\mathrm{end}}}{\theta_{\mathrm{start}} - \theta_{\mathrm{end}}} \left.\frac{\partial\mathrm{EF}}{\partial\theta}\right|_{\mathrm{trans}} \tag{2}$$

where θ_{start} and θ_{end} are the start and end soil moisture values. Whenever θ_{start} and θ_{end} are in the same soil moisture regime, $\Delta\mathrm{EF}/\Delta\theta$ is simply taken as the sensitivity $\partial\mathrm{EF}/\partial\theta$ in the respective regime. Moreover, we enforce that θ_{end} cannot be lower than θ_{wilt} since EF is zero below the wilting point.

Here $\Delta\mathrm{EF}/\Delta\theta$ is calculated for the difference between the soil moisture experiments *CTL* and *Clim20C* and, accordingly, between *CTL* and *ClimCTL*. θ_{start} and θ_{end} represent soil moisture values in two different experiments (e.g., θ_{start} in *Clim20C* and θ_{end} in *CTL*, as illustrated in Figure 1). The difference in EF is then calculated as a theoretical passage between θ_{start} and θ_{end} according to the $\mathrm{EF}(\theta)$ curve. The term $\Delta\mathrm{EF}/\Delta\theta$ is computed for each day of the investigated time period (either 20

Earth Syst. Dynam. Discuss., https://doi.org/10.5194/esd-2018-34
Manuscript under review for journal Earth Syst. Dynam.
Discussion started: 7 June 2018

or 30 years long, see Section 3.1.3) and averaged across all daily estimates. The averaged $\Delta EF/\Delta\theta$ estimate represents the *sensitivity-based* effect of soil moisture on EF.

The calculation of the sensitivity-based effect requires only input data of *CTL*. Thus, additionally to the GLACE-CMIP5 models, it can be applied to CMIP5 model output, which represents the *CTL* experiment in this case. This allows to theoretically reproduce the GLACE-CMIP5 soil moisture experiments with all 20 CMIP5 models that provide the necessary (daily) data for calculating the sensitivity-based estimates of soil moisture–climate coupling.

3.3 Estimating the soil moisture effect on temperature

3.3.1 Effect on daily maximum temperature

Due to the distinct impact of soil moisture on the magnitude of latent and sensible heat fluxes in the different soil moisture regimes, $\partial TX/\partial\theta$ is also expected to take different values in the single regimes. To quantify the effect that soil moisture shifts across the different experiments have on TX, an analogous calculation as in Eq. (2) can thus be applied, using TX instead of EF and considering the distinct sensitivities $\partial TX/\partial\theta$ in the single soil moisture regimes:

$$\frac{\Delta TX}{\Delta\theta} = \frac{\theta_{start} - \theta_{crit}}{\theta_{start} - \theta_{end}} \left.\frac{\partial TX}{\partial\theta}\right|_{wet} + \frac{\theta_{crit} - \theta_{end}}{\theta_{start} - \theta_{end}} \left.\frac{\partial TX}{\partial\theta}\right|_{trans} . \quad (3)$$

Again, soil moisture and TX data are only used from *CTL* and thus the approach can be applied to CMIP5 data as well. For the GLACE-CMIP5 models the effect can further be directly estimated from the different model experiments by performing a linear fit between the soil moisture and TX differences across the experiments, analogous to the experiment-based estimation of the soil moisture effect on EF. Multiplying $\Delta TX/\Delta\theta$ by the mean soil moisture shift between the investigated experiments yields the average effect on TX caused by the soil moisture shift (denoted δTX_θ). Additionally, we estimate the effect that shifts in the lowermost (first) percentile of the soil moisture distribution between the investigated experiments have on TX (denoted as $\delta TX_{\theta_{Q1}}$).

3.3.2 Effect on TX_x

The sensitivity-based estimates can also be used to quantify the contribution of soil moisture to the projected changes of TX_x. For this purpose we first identify the day on which TX_x occurs for each year and each grid point individually. Subsequently, the *sensitivity-based* soil moisture effect on TX is calculated by applying Eq. (3), using the sensitivity $\partial TX/\partial\theta$ from the 3-month subset that is centered on the month in which TX_x occurs and the soil moisture values in *CTL* and *Clim20C* (or *CTL* and *ClimCTL*) on the day on which TX_x occurs. Multiplying the obtained $\Delta TX/\Delta\theta$ estimate with the soil moisture shift between the two considered experiments on that day results in the theoretical soil moisture effect on TX_x. This procedure is performed for all considered years individually (that is, the 20 years surrounding a certain ΔT_{glob}), yielding 20 estimates, of which the mean is taken to get the average contribution. By subtracting these sensitivity-based TX_x contributions from ΔTX_x in *CTL*, it is possible to estimate the theoretical ΔTX_x in *Clim20C* (and accordingly in *ClimCTL*). Moreover, for the GLACE-CMIP5 models these estimates can be compared to ΔTX_x directly estimated from the experiments *Clim20C* and *ClimCTL*.

Earth Syst. Dynam. Discuss., https://doi.org/10.5194/esd-2018-34
Manuscript under review for journal Earth Syst. Dynam.
Discussion started: 7 June 2018

4 Results

Here and in the following we focus on the difference between the experiments *CTL* and *Clim20C*. The results when *CTL* and *ClimCTL* are considered instead can be found in the supplementary information.

4.1 Occurrence of soil moisture regimes

The multimodel mean temporal share of the different soil moisture regimes (based on the twelve 3-month subsets) for the GLACE-CMIP5 models and for the CMIP5 models and the regime difference between the GLACE-CMIP5 experiments *CTL* and *Clim20C* for the time period 2070–2099 are displayed in Figure 2. The regime classification for the GLACE-CMIP5 control run (Figures 2a-c) reveals that overall the wet regime has the highest share (∼56 % on global latitudinal corrected average), followed by the transitional (∼29 %) and dry regimes (∼15 %). The wet regime is mostly found in high latitudes and in tropical rainforests, which are climate zones where water is abundant. The transitional regime occurs in many regions in lower latitudes. In particular, several areas in Latin America, Africa, India, Southeast Asia, and Australia are located in the transitional regime during about half of the year. The dry regime shows the highest occurrence in deserts.

Many regions exhibit different regime shares in the two GLACE-CMIP5 experiments *CTL* and *Clim20C* (Figures 2d-f). Desert regions generally reveal an enhanced occurrence of the dry regime in *CTL* compared to *Clim20C*, which goes mostly at the expense of the transitional regime. In other regions the occurrence of the transitional regime increases in *CTL*. These hotspot regions include the southeastern United States and Mexico, central and eastern Europe, the Paraná catchment in South America, southern Africa, Southeast Asia, and eastern Australia. In the same regions the wet regime shows pronounced decreases. In high latitudes and tropical rainforests in South America and Africa the regime distributions in *CTL* and *Clim20C* only differ slightly from each other.

The CMIP5 models show a very similar soil moisture regime distribution as the analyzed GLACE-CMIP5 models in the *CTL* experiment (Figures 2g-i). This is further confirmed when considering the global share of each soil moisture regime for the single climate models (supplementary Figure S3). The four GLACE-CMIP5 models cover a similar spectrum as the 20 CMIP5 models and, thus, seem to be an appropriate CMIP5 model subset for assessing soil moisture effects on climate.

4.2 Emerging differences in soil moisture experiments

4.2.1 GLACE-CMIP5

An overview of the comparison between different key measures that characterize the effect of soil moisture on EF and TX for the time period 2070–2099 is displayed in Figure 3 as multimodel median of the GLACE-CMIP5 models. The measures are on the one side calculated directly based on the differences across the GLACE-CMIP5 experiments *CTL* and *Clim20C* (i.e., experiment-based) and, on the other side, obtained from the combination of the sensitivities in the different soil moisture regimes (i.e., sensitivity-based, see Sections 3.2 and 3.3 for details about the derivation).

Earth Syst. Dynam. Discuss., https://doi.org/10.5194/esd-2018-34
Manuscript under review for journal Earth Syst. Dynam.
Discussion started: 7 June 2018

The uppermost row (Figures 3a-c) displays the soil moisture effect on EF caused by the different soil moisture prescriptions in the two experiments *CTL* and *Clim20C*. Both the experiment-based and the sensitivity-based estimates of $\Delta\mathrm{EF}/\Delta\theta$ highlight similar regions in which soil moisture shifts evoke strong EF changes. In particular, these regions comprise the western and southern USA, Mexico, parts of Brazil, the Sahel region, southern Africa, India, Southeast Asia, and Australia. In contrast, the impact of soil moisture on EF is low in high latitudes, deserts, and tropical rainforests. The pattern correlation (calculated as Spearman rank correlation r_s) between experiment- and sensitivity-based estimates is 0.85, indicating good agreement between both estimation methods. The high correlation and the fact that the mean absolute error MAE (Figure 3c) is low compared to the actual values confirm that the sensitivity-based estimates are indeed capturing the soil moisture induced EF differences across the soil moisture experiments.

Figures 3d-f show the TX changes provoked by soil moisture shifts between the two experiments *CTL* and *Clim20C*. The negative values reflect the negative coupling between soil moisture and TX. Both the experiment-based as well as the sensitivity-based estimates of $\Delta\mathrm{TX}/\Delta\theta$ highlight similar regions with strong soil moisture effects on TX. These regions overall agree with the ones where soil moisture has a strong impact on EF, except for the Sahel region, where the effect of soil moisture on TX is weaker and Europe, where the effect is more pronounced and more widespread. The pattern correlation between the experiment-based and the sensitivity-based $\Delta\mathrm{TX}/\Delta\theta$ values is 0.59 indicating general consistency between the two approaches. Yet, the experiment-based effects of soil moisture on TX are in general stronger than the sensitivity-based effects (see differences in Figure 3f). This is particularly true for Canada, the USA, northeast Brazil, southern Africa, eastern Europe, and central Asia.

The average effect of soil moisture shifts on TX (that is $\delta\mathrm{TX}_\theta$) can be estimated by multiplying $\Delta\mathrm{TX}/\Delta\theta$ with the average soil moisture shift between the experiments *CTL* and *Clim20C*. The resulting values for $\delta\mathrm{TX}_\theta$ are displayed in Figures 3g-i. The experiment- and the sensitivity-based estimates yield similar results in South America, Africa, India, Southeast Asia, and partly in Australia. These are essentially the regions in which soil moisture shifts have an effect on EF (cf. Figures 3a-c). Especially in the Northern Hemisphere there are, however, some pronounced differences. This is reflected in the lower pattern correlation ($r_s = 0.42$) compared to the two previous measures $\Delta\mathrm{EF}/\Delta\theta$ and $\Delta\mathrm{TX}/\Delta\theta$. The experiment-based values show high effects on TX in Europe, central Asia, and partly North America, while the sensitivity-based estimates, in contrast, have lower values in eastern Europe and central Asia and exhibit a dipole structure in North America.

The impact of shifts in the lowermost (first) percentile of the soil moisture distributions in *CTL* and *Clim20C* on TX (that is $\delta\mathrm{TX}_{\theta_{\mathrm{Q1}}}$) is shown in Figures 3j-l. The soil moisture effect on $\delta\mathrm{TX}_{\theta_{\mathrm{Q1}}}$ is more pronounced than the effect on $\delta\mathrm{TX}_\theta$. This can be explained by two reasons: 1) in regions where soil moisture is predominantly in the wet regime, low soil moisture percentiles are more likely to enter the transitional regime than the mean of the distribution (see Figure 1a), and 2) the lower tails of the soil moisture distribution show a particularly strong shift between *CTL* and *Clim20C* (see Figure 1b). TX is impacted by changes of low soil moisture percentiles primarily in Europe, Canada, Brazil, southern Africa, western Australia, and some parts of central Asia, yielding values that reach up to more than 3 K. Both estimation methods agree on the overall patterns ($r_s = 0.55$). Yet, the experiment-based estimates are higher in eastern Europe and Brazil, while the sensitivity-based estimates reveal higher values in the southern USA and northern Mexico.

Earth Syst. Dynam. Discuss., https://doi.org/10.5194/esd-2018-34
Manuscript under review for journal Earth Syst. Dynam.
Discussion started: 7 June 2018

Overall, the experiment- and sensitivity-based estimates of the various measures agree rather well, in particular for $\Delta\mathrm{EF}/\Delta\theta$. Additionally, in the regions where soil moisture affects EF, both the experiment- and sensitivity-based estimates of $\delta\mathrm{TX}_{\theta}$ and $\delta\mathrm{TX}_{\theta_{\mathrm{Q1}}}$ reveal similar patterns and are of comparable strength.

4.2.2 CMIP5

Figure 4 shows the same measures as the previous section but as multimodel median obtained from the sensitivity-based estimates of the CMIP5 models. Generally, the patterns are very similar to the results for the GLACE-CMIP5 models (cf. Figure 3), but the patterns are more pronounced and overall less noisy – likely a consequence of the larger CMIP5 model ensemble (20 models) compared to GLACE-CMIP5 (4 models). Both model ensembles highlight similar regions where the soil moisture effect on EF is high (Figures 4a and 3b). In the CMIP5 models this effect is somewhat stronger in India, Southeast Asia, and the Mediterranean region. The soil moisture effects on TX (Figures 4b and 3e) are stronger in CMIP5 in the Mediterranean region, central Europe, South Africa, India, and Southeast Asia, while the GLACE-CMIP5 models show more pronounced effects in the southern USA/Mexico. For the TX differences triggered by the average soil moisture shifts between *CTL* and *Clim20C* (Figures 4c and 3h), the CMIP5 models show higher values in the southern USA/Mexico, the Mediterranean, and South Africa. TX decreases provoked by soil moisture shifts (i.e., negative TX values in Figures 4c and 3h) occur in Patagonia, eastern Africa, India, and Southeast Asia, but are less pronounced in CMIP5 compared to GLACE-CMIP5. The regions, in which changes in the first soil moisture percentile have a strong effect on TX are more confined when using the CMIP5 models (Figures 4d and 3k). They comprise mainly the southern USA/Mexico, the east side of the Andes in South America, central and eastern Europe, the Mediterranean, southern Africa, and China.

Overall, the patterns of the GLACE-CMIP5 and the CMIP5 models agree very well. However, the results should be used and interpreted cautiously in those regions, where the experiment- and sensitivity-based estimates for GLACE-CMIP5 reveal differences (Figure 3, right column; see also Section 5).

4.3 Soil moisture effect on TX_x

The soil moisture effect on TX_x calculated from the sensitivity-based estimates is displayed in Figure 5 as multimodel median for the GLACE-CMIP5 and the CMIP5 models for the model-specific time when T_{glob} increases by 1.5 K, 2.0 K, and 3.0 K with respect to preindustrial levels. Overall, the GLACE-CMIP5 models show a stronger (but more noisy) effect on TX_x than the CMIP5 models. The soil moisture contributions to TX_x become larger for higher ΔT_{glob}. Both model ensembles show strong soil moisture impacts on TX_x in the southern USA/Mexico, the Gran Chaco region in South America, southern Africa, China, and western Australia. For Europe, the CMIP5 models predict higher soil moisture effects than the GLACE-CMIP5 models. In Canada, Alaska, and Asia the GLACE-CMIP5 models reveal high values, which are, however, not confirmed by the CMIP5 models. These high values in GLACE-CMIP5 are caused by both the ACCESS and the GFDL models, which exhibit strong soil moisture shifts between the different experiments in those regions (not shown). The CMIP5 models predict a strong increase of the soil moisture effect on TX_x at higher ΔT_{glob} in the southern USA/Mexico and Europe (and to some extent also southern Africa and China), while elsewhere the impact on TX_x remains approximately constant.

Earth Syst. Dynam. Discuss., https://doi.org/10.5194/esd-2018-34
Manuscript under review for journal Earth Syst. Dynam.
Discussion started: 7 June 2018

Figure 6 shows the ΔTX_x evolution as function of ΔT_{glob} in six different SREX regions (see Section 3.1.3), in which soil moisture effects are expected to be important (e.g., Miralles et al., 2012; Schwingshackl et al., 2017; Vogel et al., 2017). The shaded areas indicate the ΔTX_x ranges directly obtained from the GLACE-CMIP5 experiments *CTL* and *Clim20C*. The red box-and-whisker plots represent 20-year average ΔTX_x distributions in *CTL* around the indicated T_{glob} levels. To account for the effect that soil moisture shifts between *CTL* and *Clim20C* have on TX_x, the sensitivity-based soil moisture effect on TX_x is subtracted from the 20-year average ΔTX_x (see Section 3.3.2). The resulting soil moisture effect-corrected ΔTX_x is represented by the blue box-and-whisker plots. For *CTL* the experiment-based estimates reveal a faster increase for ΔTX_x than for ΔT_{glob} – a characteristic that was also shown by Seneviratne et al. (2016) and Vogel et al. (2017). However, when soil moisture is prescribed according to *Clim20C* (blue range), the excess increase is almost completely offset (cf. Vogel et al., 2017). The sensitivity-based ΔTX_x estimates also show a slower increase of TX_x for *Clim20C* (blue box-and-whisker plots) compared to *CTL* (red box-and-whisker plots). In central North America, the Amazon, the Mediterranean, southern Africa, and northern Australia the sensitivity-based and the experiment-based ΔTX_x estimates are in good agreement. Yet, the sensitivity-based estimates generally exhibit a smaller difference between *CTL* and *Clim20C* than the experiment-based estimates. In contrast to the good agreement in these regions, for central Europe the soil moisture effect calculated from the sensitivity-based estimates yields much weaker impacts than the experiment-based effect on ΔTX_x.

An overview of ΔTX_x in *CTL* and *Clim20C* using the sensitivity-based estimates for both GLACE-CMIP5 and CMIP5 is shown in Figure 7. Generally, both model sets give similar results. Especially in the Amazon and central Europe, the CMIP5 and the GLACE-CMIP5 estimations agree well. Yet, they also reveal differences in some regions. The CMIP5 models exhibit a narrower spread than GLACE-CMIP5 in central North America and the Mediterranean. In southern Africa and northern Australia the ΔTX_x spread of CMIP5 is larger than the one of GLACE-CMIP5. In central North America and southern Africa the CMIP5 models show on average stronger soil moisture effects on TX_x than the GLACE-CMIP5 models, while in northern Australia the effects are lower.

5 Discussion

Estimating the effect of soil moisture on EF and TX based on the sensitivities in the single soil moisture regimes constitutes a simple and powerful tool to evaluate how soil moisture shifts across the different GLACE-CMIP5 experiments affect soil misture–climate coupling. Because the soil moisture evolution is the only imposed difference between the GLACE-CMIP5 experiments *CTL*, *Clim20C*, and *ClimCTL*, the resulting climate effects can be directly attributed to differences in soil moisture. The possibility to establish this causal link is a main advantage of the idealized GLACE-CMIP5 experiments. The good agreement between the experiment- and sensitivity-based estimates of the soil moisture effects on EF is also an indirect validation of the applied $EF(\theta)$ framework and gives confidence that it is able to represent cause-effect relations of soil moisture–climate coupling.

To obtain the sensitivity-based estimates no other model data than the CMIP5 standard output is required. The methodology can thus be used to estimate soil moisture–climate coupling without the need of performing additional model simulations.

Earth Syst. Dynam. Discuss., https://doi.org/10.5194/esd-2018-34
Manuscript under review for journal Earth Syst. Dynam.
Discussion started: 7 June 2018

Especially for investigating the soil moisture control on EF, the sensitivity-based estimates seem to give reliable results, as can be seen from the comparison with the experiment-based estimates in Figure 3a-c. Additionally, in the regions where soil moisture effects on EF are particularly pronounced, both the experiment- and the sensitivity-based estimates of $\delta\mathrm{TX}_{\theta}$ and $\delta\mathrm{TX}_{\theta_{\mathrm{Q1}}}$ agree well. This is a strong indication that in these regions the different soil moisture prescriptions in the GLACE-CMIP5 experiments affect TX directly by affecting EF, that is by the soil moisture control on the partitioning of net radiation into latent and sensible heat fluxes.

Yet, there are some regions where the experiment-based and the sensitivity-based estimates of soil moisture–climate coupling disagree. There are two possible explanations for this. The first is based on the regime classification, which is central for calculating the sensitivity-based estimates. If soil moisture enters a certain regime only rarely, the regime classification might not be sensitive enough to distinguish this regime from the predominant one and the rare regime could thus be missed. As a result, the sensitivities $\partial\mathrm{EF}/\partial\theta$ might be over- or underestimated yielding biased estimates for the average effect on EF (and similarly on TX). Secondly, prescribing soil moisture in the GLACE-CMIP5 experiments might not only influence the heat fluxes, but also lead to secondary effects caused by other soil moisture feedbacks. Berg et al. (2014) showed, for instance, that for the soil moisture experiments conducted with the GFDL model in addition to latent heat flux also leaf area index, cloud cover, and potential evaporation differ between the single experiments. As long as these effects feed back on evapotranspiration, they can in principal be captured by the $\mathrm{EF}(\theta)$ framework. However, the complex coupling between the land surface and the atmosphere can generate additional nonlinearities beyond the presence of a critical soil moisture threshold for evapotranspiration (Figure 1a) and, thus, influence the atmosphere by processes that are not taken into account by the $\mathrm{EF}(\theta)$ framework.

Another important and maybe even more relevant aspect are non-local soil moisture effects on the atmosphere (e.g., Seneviratne et al., 2013; Koster et al., 2014). For instance, thermal advection could be responsible for transporting temperature signals to regions downwind of the ones that experience strong local soil moisture–climate coupling (Seneviratne et al., 2013). Differences in the patterns between the sensitivity-based estimates (which measure the local soil moisture–climate coupling strength) and the experiment-based estimates (which include both local and non-local effects) might thus give an indication about remote effects caused by soil moisture shifts. For example, the stronger TX signal in the experiment-based estimates in central North America and Eastern Europe/Central Asia (Figures 3g-i) indicate that westerlies transport the soil moisture signal from the US West Coast and Europe towards the east.

In several regions, the effect of soil moisture shifts on EF is connected to regime shifts between the different soil moisture experiments (see Figures 2d-f and 3). The effect on EF is however not only limited to the regions that exhibit regime shifts between the soil moisture experiments; also soil moisture changes within one soil moisture regime have an impact on climate. Moreover, the strong dependency of EF on soil moisture is not necessarily translated into effects on TX, as can for example be seen in the Sahel region, where soil moisture impacts EF but effects on TX are rather low. A region with particularly high impacts of soil moisture on TX is Europe. This region is of special interest because the experiment-based effect on TX clearly exceeds the sensitivity-based one (Figures 3g-l), although Europe shows different soil moisture regime shares in the experiments *CTL* and *Clim20C* (Figure 2d-f) and, thus, one would expect that the sensitivity-based estimates show a strong

effect on TX. As discussed above, the discrepancy between the experiment- and sensitivity-based estimates points to additional feedbacks (like circulation changes or soil moisture–precipitation feedbacks) that are not captured by the sensitivity-based estimation, but might be important for soil moisture–temperature coupling in Europe.

The effect of soil moisture on TX is in general expected to be strongest for extreme conditions (Hirschi et al., 2011; Fischer and Schär, 2009; Seneviratne et al., 2016; Vogel et al., 2017). This is confirmed by our results showing a larger effect of shifts of the first soil moisture percentile than for mean soil moisture shifts (Figures 3g-l and 4c-d) as well as pronounced impacts on TX_x (Figure 5). However, the results have to be interpreted with some caution, since the soil moisture experiments *Clim20C* and *ClimCTL* are limited to prescribed soil moisture climatologies and have thus different soil moisture distributions than *CTL* what affects primarily the tails of the soil moisture distributions. Moreover, wrong soil moisture regime classifications – and, thus, wrong sensitivity estimations – affect the results more strongly during very low soil moisture conditions than during average soil moisture conditions. Since soil moisture impacts extremes mostly during low soil moisture conditions, the estimated soil moisture contributions to TX_x are especially affected by possible wrong sensitivity estimations.

Soil moisture effects on TX_x are particularly strong in the southern USA/Mexico, Europe, and western Australia. Vogel et al. (2017), whose results we try to confirm here by calculating soil moisture contributions to TX_x from the sensitivity-based estimates, showed that soil moisture contributes an important part for explaining the large TX_x increases in those regions. The results of the present study are in agreement with the conclusions of Vogel et al. (2017). Note that the two studies do not use the exactly same GLACE-CMIP5 model (sub-)ensemble and, therefore, their results reveal some marginal differences.

While in many regions the sensitivity-based soil moisture effects on TX_x yield similar results as the ones directly obtained from the GLACE-CMIP5 experiments (Figure 6), there are large differences especially for central Europe, where the sensitivity-based estimates predict a smaller soil moisture effect than the ones directly estimated from the GLACE-CMIP5 experiments. Again, this fact hints to some secondary feedbacks triggered by soil moisture shifts between the GLACE-CMIP5 experiments. These secondary effects on TX_x seem to be largest in Europe, while in the other investigated regions the direct soil moisture effect explains most of the observed differences.

All the sensitivity-based estimates for GLACE-CMIP5 can be either obtained with soil moisture climatologies calculated according to the GLACE-CMIP5 protocol or with soil moisture directly taken from the respective GLACE-CMIP5 soil moisture experiments. Here we use the former approach to be consistent with the calculation for the CMIP5 models. In general, the results are similar independent of the soil moisture choice for GLACE-CMIP5. Only in the Amazon and in southern Africa the ΔTX_x spread is enhanced when using soil moisture directly from the GLACE-CMIP5 runs (not shown). The reason for this might be the unintended soil moisture shift in ACCESS in *Clim20C* (see Section 3.1.1).

When considering the differences between *CTL* and the transient soil moisture climatology *ClimCTL* (supplementary Figures S5-S9), the soil moisture effect on TX and TX_x is not as strong as for the difference between *CTL* and *Clim20C*. Only in middle-to-high latitudes in the Northern Hemisphere (particularly in the USA, Europe, and China) there are some impacts on TX but they are considerably smaller than the effects in *Clim20C*. This confirms the finding of Vogel et al. (2017) that soil moisture impacts on extreme temperatures are due to long-term soil moisture trends rather than to changes in soil moisture variability alone.

Earth Syst. Dynam. Discuss., https://doi.org/10.5194/esd-2018-34
Manuscript under review for journal Earth Syst. Dynam.
Discussion started: 7 June 2018

6 Conclusions

In this study we analyze the effect that different soil moisture prescriptions in the single GLACE-CMIP5 experiments have on evaporative fraction EF and daily maximum near-surface air temperature TX. The analysis is based on an idealized framework (Figure 1a) that describes the relation between soil moisture θ and EF by considering different soil moisture regimes (Koster et al., 2009; Seneviratne et al., 2010). This framework was found to be well suited to quantify the impact of soil moisture on heat fluxes and daily maximum near-surface air temperature (Schwingshackl et al., 2017), highlighting its applicability for studying soil moisture–climate coupling.

Using a theoretical approach based on the different sensitivities of EF and TX to soil moisture in the single soil moisture regimes, soil moisture–climate coupling in the GLACE-CMIP5 experiments can be quantified and explained. In particular, the effect of soil moisture shifts on EF and TX across GLACE-CMIP5 experiments can be reproduced (Figure 3). Especially for the soil moisture impact on EF, the sensitivity-based estimates agree very well with estimations of the coupling strength calculated directly from the GLACE-CMIP5 soil moisture experiments. Moreover, in regions where soil moisture exerts control on latent heat fluxes, the impact of soil moisture on TX is reliably reproduced by the sensitivity-based estimates. Additionally, differences between the sensitivity- and the experiment-based estimates give an indication about non-local climate effects that are caused by soil moisture shifts between the different GLACE-CMIP5 experiments. The sensitivity-based approach constitutes thus a powerful method to assess soil moisture–climate coupling in the GLACE-CMIP5 experiments. Furthermore, the good agreement between the experiment- and sensitivity-based estimates of the soil moisture effects gives confidence that the used approach based on the EF(θ) framework is able to represent cause-effect relations of soil moisture–climate coupling. Since the sensitivity-based estimates only require input data from the control run (i.e., no additional simulations), the method can be applied directly to CMIP5 models. The obtained patterns of strong soil moisture–climate coupling for CMIP5 are in accordance with the ones estimated with GLACE-CMIP5 (Figure 4). Moreover, the larger CMIP5 model ensemble increases reliability and robustness of the calculated soil moisture effects on EF and TX.

Eventually, the soil moisture contributions to the yearly maximum value of daily maximum temperature TX_x are quantified using the sensitivity-based estimates (Figures 5-7). The results highlight the important impact of soil moisture on TX_x in various regions on Earth. While in most of the investigated regions the sensitivity- and experiment-based estimations of the soil moisture contributions to TX_x agree, in central Europe the soil moisture contribution to TX_x calculated from the sensitivity-based estimates is lower than the one directly obtained from the different GLACE-CMIP5 experiments. This points to secondary effects of soil moisture prescriptions on circulation, precipitation, and cloud cover (Seneviratne et al., 2013; Berg et al., 2015) that seem to be important, for example, in central Europe.

The presented theoretical approach using sensitivity-based estimates to quantify soil moisture–climate coupling in GLACE-CMIP5 constitutes a well suited tool that can be applied without the need of specific soil moisture prescription experiments. Additionally, it can easily be applied to CMIP5 models to emulate GLACE-style soil moisture prescription in regions where local soil moisture–atmosphere feedbacks dominate. It provides thus an option to avoid costly climate model experiments and can be applied to various climate model environments for quantifying the soil moisture–climate coupling strength.

Data availability. GLACE-CMIP5 data are hosted at ETH Zürich and are available upon request (see http://www.iac.ethz.ch/group/land-climate-dynamics/research/glace-cmip.html). CMIP5 data can be downloaded at https://esgf-node.llnl.gov/search/cmip5.

Author contributions. C.S. conducted the analysis and wrote the manuscript. M.H. gave significant input during the method implementation and provided feedback on the manuscript. S.I.S. contributed the initial idea for the study, gave input on the used methods and provided funding.

Competing interests. The authors declare that they do not have any competing interests.

Acknowledgements. We thank Kirsten Findell, Wilhelm May, and Stefan Hagemann for constructive feedback on the manuscript. This study was supported by the European Research Council (ERC) "DROUGHT-HEAT" project funded through the European Community's Seventh Framework Programme (grant agreement FP7-IDEAS-ERC-617518). We acknowledge the World Climate Research Programme's Working Group on Coupled Modelling, which is responsible for CMIP, and we thank the climate modeling groups (listed in supplementary Table S1) for producing and making available their model output. For CMIP the U.S. Department of Energy's Program for Climate Model Diagnosis and Intercomparison provides coordinating support and led development of software infrastructure in partnership with the Global Organization for Earth System Science Portals. We thank GEWEX (World Climate Research Programme, WCRP) and iLEAPS (Integrated Geosphere-Biosphere Programme, IGBP) projects for the coordination and realization of the GLACE-CMIP5 experiment and Alexis Berg, Frederique Cheruy, Stefan Hagemann, David Lawrence, Ruth Lorenz, Arndt Meier, Anna Ukkola, and Bart van den Hurk for providing the GLACE-CMIP5 simulations.

References

Berg, A., Lintner, B. R., Findell, K. L., Malyshev, S., Loikith, P. C., and Gentine, P.: Impact of Soil Moisture–Atmosphere Interactions on Surface Temperature Distribution, Journal of Climate, 27, 7976–7993, https://doi.org/10.1175/JCLI-D-13-00591.1, 2014.

Berg, A., Lintner, B. R., Findell, K., Seneviratne, S. I., van den Hurk, B., Ducharne, A., Chéruy, F., Hagemann, S., Lawrence, D. M., Malyshev, S., et al.: Interannual coupling between summertime surface temperature and precipitation over land: Processes and implications for climate change, Journal of Climate, 28, 1308–1328, https://doi.org/10.1175/JCLI-D-14-00324.1, 2015.

Berg, A., Findell, K., Lintner, B., Giannini, A., Seneviratne, S. I., Van Den Hurk, B., Lorenz, R., Pitman, A., Hagemann, S., Meier, A., et al.: Land–atmosphere feedbacks amplify aridity increase over land under global warming, Nature Climate Change, 6, 869+, https://doi.org/10.1038/NCLIMATE3029, 2016.

Berg, A., Sheffield, J., and Milly, P. C.: Divergent surface and total soil moisture projections under global warming, Geophysical Research Letters, 44, 236–244, https://doi.org/10.1002/2016GL071921, 2017.

Casagrande, E., Mueller, B., Miralles, D. G., Entekhabi, D., and Molini, A.: Wavelet correlations to reveal multiscale coupling in geophysical systems, Journal of Geophysical Research: Atmospheres, 120, 7555–7572, https://doi.org/10.1002/2015JD023265, 2015.

de Jeu, R. A. M., Wagner, W., Holmes, T. R. H., Dolman, A. J., van de Giesen, N. C., and Friesen, J.: Global Soil Moisture Patterns Observed by Space Borne Microwave Radiometers and Scatterometers, Surveys in Geophysics, 29, 399–420, https://doi.org/10.1007/s10712-008-9044-0, 2008.

Dirmeyer, P. A.: The terrestrial segment of soil moisture–climate coupling, Geophysical Research Letters, 38, https://doi.org/10.1029/2011GL048268, 2011.

Dorigo, W., Wagner, W., Hohensinn, R., Hahn, S., Paulik, C., Xaver, A., Gruber, A., Drusch, M., Mecklenburg, S., Oevelen, P. v., et al.: The International Soil Moisture Network: a data hosting facility for global in situ soil moisture measurements, Hydrology and Earth System Sciences, 15, 1675–1698, https://doi.org/10.5194/hess-15-1675-2011, 2011.

Dorigo, W., Wagner, W., Albergel, C., Albrecht, F., Balsamo, G., Brocca, L., Chung, D., Ertl, M., Forkel, M., Gruber, A., et al.: ESA CCI Soil Moisture for improved Earth system understanding: state-of-the art and future directions, Remote Sensing of Environment, 203, 185–215, https://doi.org/10.1016/j.rse.2017.07.001, 2017.

Fischer, E. M. and Schär, C.: Future changes in daily summer temperature variability: driving processes and role for temperature extremes, Climate Dynamics, 33, 917, https://doi.org/10.1007/s00382-008-0473-8, 2009.

Hauser, M., Orth, R., and Seneviratne, S. I.: Role of soil moisture vs. recent climate change for the 2010 heat wave in western Russia, Geophysical Research Letters, 43, 2819–2826, https://doi.org/10.1002/2016GL068036, 2016.

Hirschi, M., Seneviratne, S. I., Alexandrov, V., Boberg, F., Boroneant, C., Christensen, O. B., Formayer, H., Orlowsky, B., and Stepanek, P.: Observational evidence for soil-moisture impact on hot extremes in southeastern Europe, Nature Geoscience, 4, 17–21, https://doi.org/10.1038/ngeo1032, 2011.

Hirschi, M., Meuller, B., Dorigo, W., and Seneviratne, S. I.: Using remotely sensed soil moisture for land–atmosphere coupling diagnostics: The role of surface vs. root-zone soil moisture variability, Remote Sensing of Environment, 154, 246–252, https://doi.org/10.1016/j.rse.2014.08.030, 2014.

Koster, R., Schubert, S., and Suarez, M.: Analyzing the concurrence of meteorological droughts and warm periods, with implications for the determination of evaporative regime, Journal of Climate, 22, 3331–3341, https://doi.org/10.1175/2008JCLI2718.1, 2009.

Koster, R. D., Suarez, M. J., and Heiser, M.: Variance and Predictability of Precipitation at Seasonal-to-Interannual Timescales, Journal of Hydrometeorology, 1, 26–46, https://doi.org/10.1175/1525-7541(2000)001<0026:VAPOPA>2.0.CO;2, 2000.

Koster, R. D., Dirmeyer, P. A., Guo, Z., Bonan, G., Chan, E., Cox, P., Gordon, C., Kanae, S., Kowalczyk, E., Lawrence, D., et al.: Regions of strong coupling between soil moisture and precipitation, Science, 305, 1138–1140, https://doi.org/10.1126/science.1100217, 2004.

Koster, R. D., Sud, Y. C., Guo, Z., Dirmeyer, P. A., Bonan, G., Oleson, K. W., Chan, E., Verseghy, D., Cox, P., Davies, H., Kowalczyk, E., Gordon, C. T., Kanae, S., Lawrence, D., Liu, P., Mocko, D., Lu, C.-H., Mitchell, K., Malyshev, S., McAvaney, B., Oki, T., Yamada, T., Pitman, A., Taylor, C. M., Vasic, R., and Xue, Y.: GLACE: The Global Land–Atmosphere Coupling Experiment. Part I: Overview, Journal of Hydrometeorology, 7, 590–610, https://doi.org/10.1175/JHM510.1, 2006.

Koster, R. D., Mahanama, S. P. P., Yamada, T. J., Balsamo, G., Berg, A. A., Boisserie, M., Dirmeyer, P. A., Doblas-Reyes, F. J., Drewitt, G., Gordon, C. T., Guo, Z., Jeong, J.-H., Lawrence, D. M., Lee, W.-S., Li, Z., Luo, L., Malyshev, S., Merryfield, W. J., Seneviratne, S. I., Stanelle, T., van den Hurk, B. J. J. M., Vitart, F., and Wood, E. F.: Contribution of land surface initialization to subseasonal forecast skill: First results from a multi-model experiment, Geophysical Research Letters, 37, https://doi.org/10.1029/2009GL041677, 2010.

Koster, R. D., Chang, Y., and Schubert, S. D.: A Mechanism for Land–Atmosphere Feedback Involving Planetary Wave Structures, Journal of Climate, 27, 9290–9301, https://doi.org/10.1175/JCLI-D-14-00315.1, 2014.

Lorenz, R., Pitman, A. J., Hirsch, A. L., and Srbinovsky, J.: Intraseasonal versus interannual measures of land–atmosphere coupling strength in a global climate model: GLACE-1 versus GLACE-CMIP5 experiments in ACCESS1.3b, Journal of Hydrometeorology, 16, 2276–2295, https://doi.org/10.1175/JHM-D-14-0206.1, 2015.

Lorenz, R., Argüeso, D., Donat, M. G., Pitman, A. J., van den Hurk, B., Berg, A., Lawrence, D. M., Chéruy, F., Ducharne, A., Hagemann, S., Meier, A., Milly, P. C. D., and Seneviratne, S. I.: Influence of land-atmosphere feedbacks on temperature and precipitation extremes in the GLACE-CMIP5 ensemble, Journal of Geophysical Research: Atmospheres, 121, 607–623, https://doi.org/10.1002/2015JD024053, 2016.

May, W., Meier, A., Rummukainen, M., Berg, A., Chéruy, F., and Hagemann, S.: Contributions of soil moisture interactions to climate change in the tropics in the GLACE–CMIP5 experiment, Climate dynamics, 45, 3275–3297, https://doi.org/10.1007/s00382-015-2538-9, 2015.

Miralles, D., den Berg, M. v., Teuling, A., and Jeu, R. d.: Soil moisture-temperature coupling: A multiscale observational analysis, Geophysical Research Letters, 39, https://doi.org/10.1029/2012GL053703, 2012.

Miralles, D. G., Teuling, A. J., van Heerwaarden, C. C., and de Arellano, J. V.-G.: Mega-heatwave temperatures due to combined soil desiccation and atmospheric heat accumulation, Nature Geoscience, 7, 345–349, https://doi.org/10.1038/ngeo2141, 2014.

Mueller, B. and Seneviratne, S. I.: Hot days induced by precipitation deficits at the global scale, Proceedings of the national academy of sciences, 109, 12 398–12 403, https://doi.org/10.1073/pnas.1204330109, 2012.

Riahi, K., Rao, S., Krey, V., Cho, C., Chirkov, V., Fischer, G., Kindermann, G., Nakicenovic, N., and Rafaj, P.: RCP 8.5–A scenario of comparatively high greenhouse gas emissions, Climatic Change, 109, 33, https://doi.org/10.1007/s10584-011-0149-y, 2011.

Santanello, J. A., Peters-Lidard, C. D., and Kumar, S. V.: Diagnosing the Sensitivity of Local Land–Atmosphere Coupling via the Soil Moisture–Boundary Layer Interaction, Journal of Hydrometeorology, 12, 766–786, https://doi.org/10.1175/JHM-D-10-05014.1, 2011.

Santanello, J. A., Roundy, J., and Dirmeyer, P. A.: Quantifying the Land–Atmosphere Coupling Behavior in Modern Reanalysis Products over the U.S. Southern Great Plains, Journal of Climate, 28, 5813–5829, https://doi.org/10.1175/JCLI-D-14-00680.1, 2015.

Schwingshackl, C., Hirschi, M., and Seneviratne, S. I.: Quantifying Spatiotemporal Variations of Soil Moisture Control on Surface Energy Balance and Near-Surface Air Temperature, Journal of Climate, 30, 7105–7124, https://doi.org/10.1175/JCLI-D-16-0727.1, 2017.

Seneviratne, S. I., Lüthi, D., Litschi, M., and Schär, C.: Land–atmosphere coupling and climate change in Europe, Nature, 443, 205–209, https://doi.org/10.1038/nature05095, 2006.

Seneviratne, S. I., Corti, T., Davin, E. L., Hirschi, M., Jaeger, E. B., Lehner, I., Orlowsky, B., and Teuling, A. J.: Investigating soil moisture–climate interactions in a changing climate: A review, Earth-Science Reviews, 99, 125–161, https://doi.org/10.1016/j.earscirev.2010.02.004, 2010.

Seneviratne, S. I., Nicholls, N., Easterling, D., Goodess, C. M., Kanae, S., Kossin, J., Luo, Y., Marengo, J., McInnes, K., Rahimi, M., Reichstein, M., Sorteberg, A., Vera, C., and Zhang, X.: Changes in Climate Extremes and their Impacts on the Natural Physical Environmenty, in: Managing the Risks of Extreme Events and Disasters to Advance Climate Change Adaptation. A Special Report of Working Groups I and II of the Intergovernmental Panel on Climate Change (IPCC), edited by Field, C. B., Barros, V., Stocker, T. F., Qin, D., Dokken, D. J., Ebi, K. L., Mastrandrea, M. D., Mach, K. J., Plattner, G.-K., Allen, S. K., Tignor, M., and Midgley, P. M., pp. 109–230, Cambridge University Press, Cambridge, United Kingdom and New York, NY, USA, 2012.

Seneviratne, S. I., Wilhelm, M., Stanelle, T., Hurk, B., Hagemann, S., Berg, A., Cheruy, F., Higgins, M. E., Meier, A., Brovkin, V., et al.: Impact of soil moisture-climate feedbacks on CMIP5 projections: First results from the GLACE-CMIP5 experiment, Geophysical Research Letters, 40, 5212–5217, https://doi.org/10.1002/grl.50956, 2013.

Seneviratne, S. I., Donat, M. G., Pitman, A. J., Knutti, R., and Wilby, R. L.: Allowable CO_2 emissions based on regional and impact-related climate targets, Nature, 529, 477–483, https://doi.org/10.1038/nature16542, 2016.

Sippel, S., Zscheischler, J., Mahecha, M. D., Orth, R., Reichstein, M., Vogel, M., and Seneviratne, S. I.: Refining multi-model projections of temperature extremes by evaluation against land–atmosphere coupling diagnostics, Earth System Dynamics, 8, 387–403, https://doi.org/10.5194/esd-8-387-2017, 2017.

Taylor, K. E., Stouffer, R. J., and Meehl, G. A.: An overview of CMIP5 and the experiment design, Bulletin of the American Meteorological Society, 93, 485–498, https://doi.org/10.1175/BAMS-D-11-00094.1, 2012.

Teuling, A., Hirschi, M., Ohmura, A., Wild, M., Reichstein, M., Ciais, P., Buchmann, N., Ammann, C., Montagnani, L., Richardson, A., et al.: A regional perspective on trends in continental evaporation, Geophysical Research Letters, 36, https://doi.org/10.1029/2008GL036584, 2009.

van den Hurk, B., Best, M., Dirmeyer, P., Pitman, A., Polcher, J., and Santanello, J.: Acceleration of land surface model development over a decade of GLASS, Bulletin of the American Meteorological Society, 92, 1593–1600, https://doi.org/10.1175/BAMS-D-11-00007.1, 2011.

Vogel, M. M., Orth, R., Cheruy, F., Hagemann, S., Lorenz, R., Hurk, B., and Seneviratne, S. I.: Regional amplification of projected changes in extreme temperatures strongly controlled by soil moisture-temperature feedbacks, Geophysical Research Letters, 44, 1511–1519, https://doi.org/10.1002/2016GL071235, 2017.

Whan, K., Zscheischler, J., Orth, R., Shongwe, M., Rahimi, M., Asare, E. O., and Seneviratne, S. I.: Impact Of Soil Moisture On Extreme Maximum Temperatures In Europe, Weather and Climate Extremes, 9, 57–67, https://doi.org/10.1016/j.wace.2015.05.001, 2015.

Wilks, D. S.: "The stippling shows statistically significant gridpoints": How Research Results are Routinely Overstated and Overinterpreted, and What to Do about It, Bulletin of the American Meteorological Society, 97, 2263–2273, https://doi.org/10.1175/BAMS-D-15-00267.1, 2016.

Zscheischler, J., Orth, R., and Seneviratne, S. I.: A submonthly database for detecting changes in vegetation-atmosphere coupling, Geophysical Research Letters, 42, 9816–9824, https://doi.org/10.1002/2015GL066563, 2015.

Earth Syst. Dynam. Discuss., https://doi.org/10.5194/esd-2018-34
Manuscript under review for journal Earth Syst. Dynam.
Discussion started: 7 June 2018

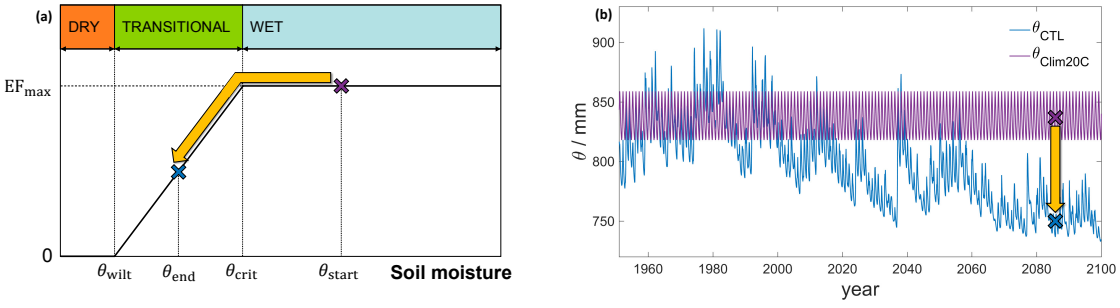

Figure 1. (a) Conceptual framework for the dependence of evaporative fraction EF on soil moisture θ and classification of the different soil moisture regimes (adapted from Seneviratne et al., 2010). θ_{wilt} is the wilting point and θ_{crit} the critical point. (b) Example of soil moisture evolution in the GLACE-CMIP5 control run (θ_{CTL}) and the run with prescribed 1971–2000 soil moisture climatology ($\theta_{Clim20C}$) in EC-EARTH at a grid point close to Jerusalem. For illustration purposes, two soil moisture values (shown as violet and blue crosses) representing soil moisture values in θ_{CTL} and $\theta_{Clim20C}$ are indicated. The shift in soil moisture between the experiments could potentially lead to a change in soil moisture regimes (yellow arrow in a) and, thus, to a nonlinear change in EF.

Earth Syst. Dynam. Discuss., https://doi.org/10.5194/esd-2018-34
Manuscript under review for journal Earth Syst. Dynam.
Discussion started: 7 June 2018

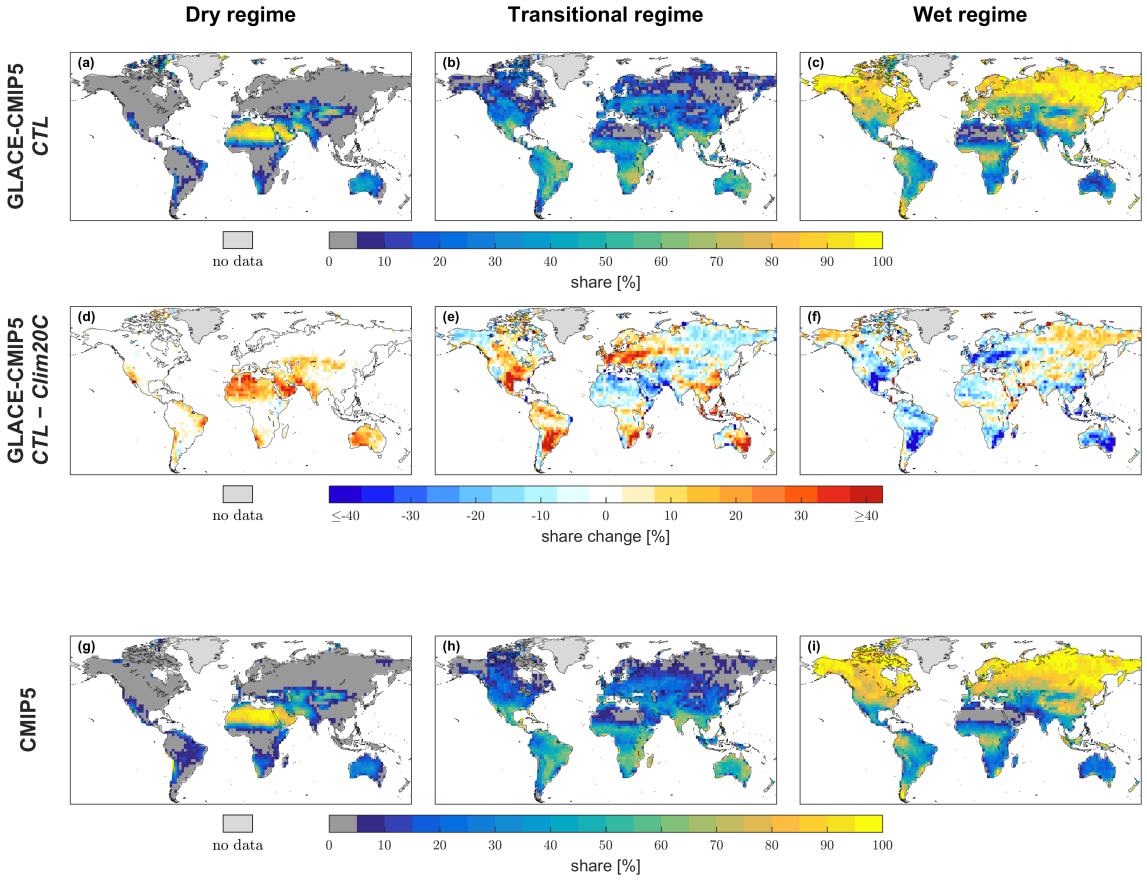

Figure 2. (a)-(c) Multimodel mean occurrence of the different soil moisture regimes in the GLACE-CMIP5 control run (*CTL*) for the time period 2070–2099. The percentages indicate how many of the 3-month subsets are located in each regime in the course of the year. (Note that the number of 3-month subsets on a grid point might be less than twelve since we require that all involved variables for calculating EF are positive. This restriction affects primarily grid cells at high latitudes, see Schwingshackl et al. (2017) for more details.) All 3-month subsets that include passages between the transitional regime and another regime are assigned to the transitional regime occurrence. (d)-(f) Difference in soil moisture regime occurrence in GLACE-CMIP5 between the control run (*CTL*) and the run with prescribed 1971–2000 soil moisture climatology (*Clim20C*). (g)-(i) Multimodel mean occurrence of the different soil moisture regimes in the CMIP5 models for the time period 2070–2099.

Earth Syst. Dynam. Discuss., https://doi.org/10.5194/esd-2018-34
Manuscript under review for journal Earth Syst. Dynam.
Discussion started: 7 June 2018

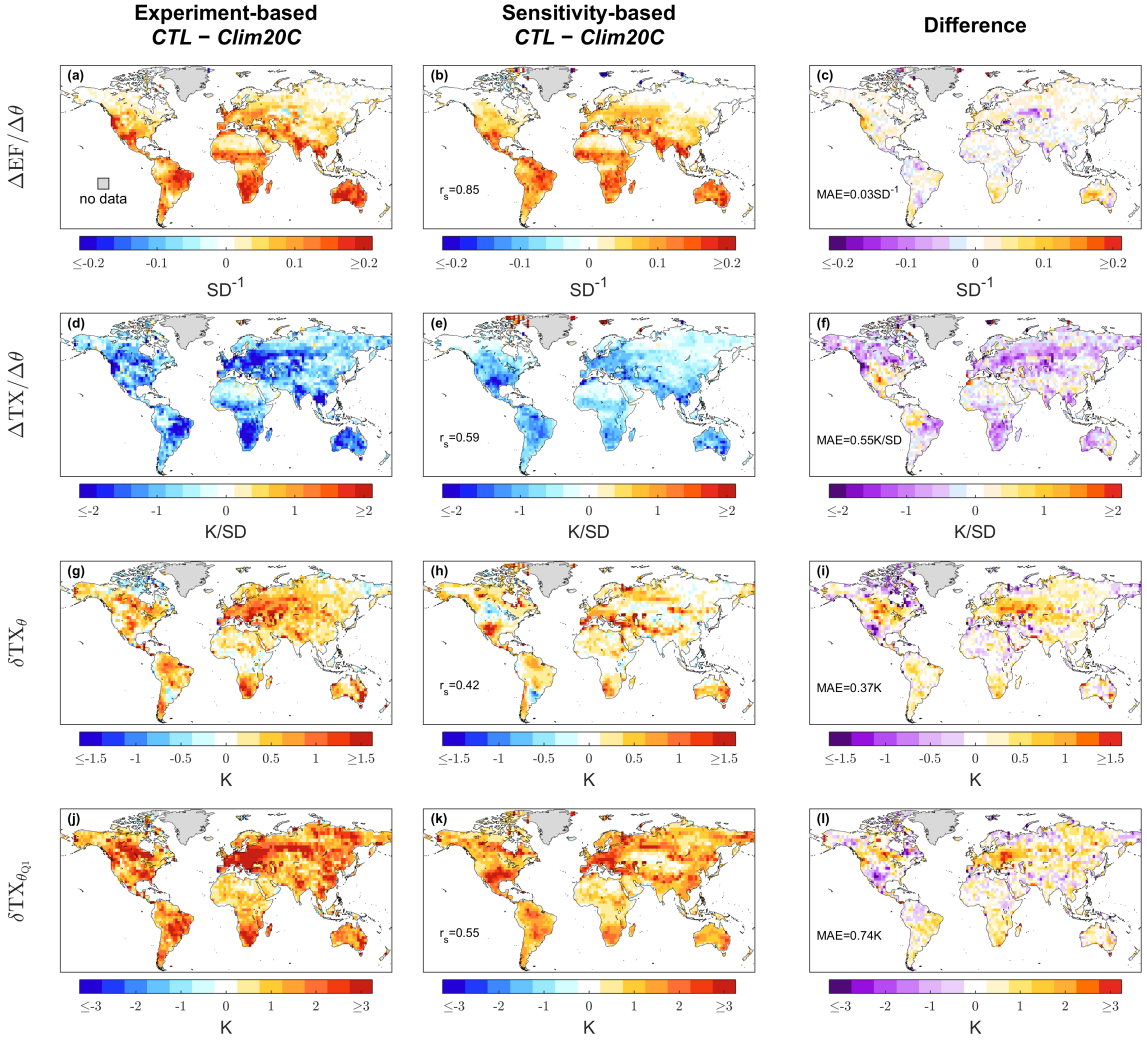

Figure 3. Multimodel median of the GLACE-CMIP5 models for different key measures used to quantify the difference between the soil moisture experiments *CTL* and *Clim20C*. (Left) Experiment-based estimates, (center) sensitivity-based estimates, and (right) difference between both estimates. The different rows show (a)-(c) the effect of changes in soil moisture θ on evaporative fraction EF and (d)-(f) on daily maximum near-surface air temperature TX, (g)-(i) the change of TX caused by the mean shift of soil moisture θ between *CTL* and *Clim20C*, and (j)-(l) the TX change when considering the shift between the lowermost (first) percentile of the soil moisture distributions in *CTL* and *Clim20C*. The values are averaged over all 3-month subsets. For each 3-month subset and each climate model, grid cells where the p values of the linear regression coefficient used to calculate the experiment-based estimates (left column) are not significant are masked (the p values were adjusted according to Wilks, 2016). The numbers in the central column indicate the pattern correlation (Spearman rank coefficient r_s) between the experiment- and sensitivity-based estimates. The numbers in the right column indicate the mean absolute error (MAE) between both estimation methods.

Earth Syst. Dynam. Discuss., https://doi.org/10.5194/esd-2018-34
Manuscript under review for journal Earth Syst. Dynam.
Discussion started: 7 June 2018

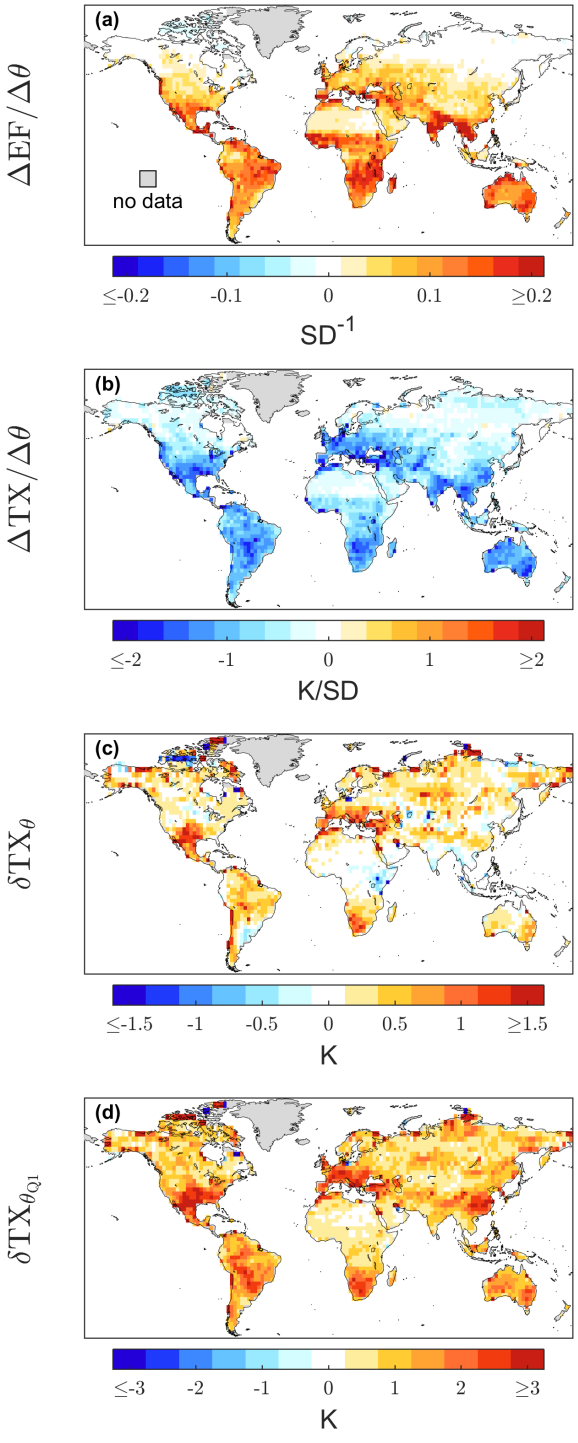

Figure 4. As in Figure 3 (central column), that is the sensitivity-based estimates, but for the CMIP5 multimodel median.

Earth Syst. Dynam. Discuss., https://doi.org/10.5194/esd-2018-34
Manuscript under review for journal Earth Syst. Dynam.
Discussion started: 7 June 2018

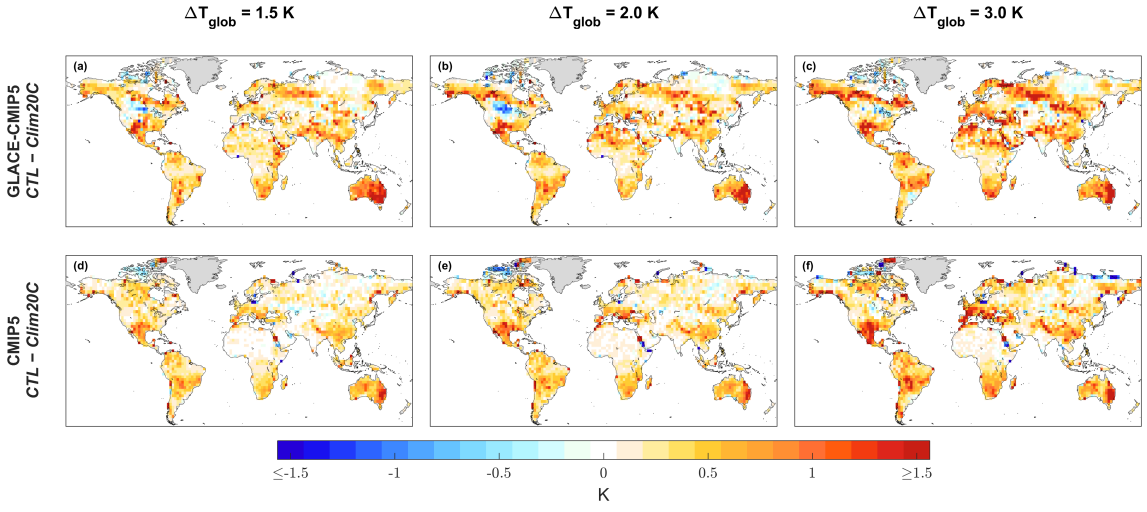

Figure 5. Multimodel median of the soil moisture contribution to the yearly maximum value of daily maximum temperature TX_x calculated from the soil moisture difference between *CTL* and *Clim20C* in GLACE-CMIP5 (upper row) and CMIP5 models (lower row) using the sensitivity-based estimates. The different columns show the soil moisture contribution to TX_x when global mean temperature increase ΔT_{glob} reaches (left) 1.5 K, (center) 2.0 K, and (right) 3.0 K above preindustrial temperature levels.

Earth Syst. Dynam. Discuss., https://doi.org/10.5194/esd-2018-34
Manuscript under review for journal Earth Syst. Dynam.
Discussion started: 7 June 2018

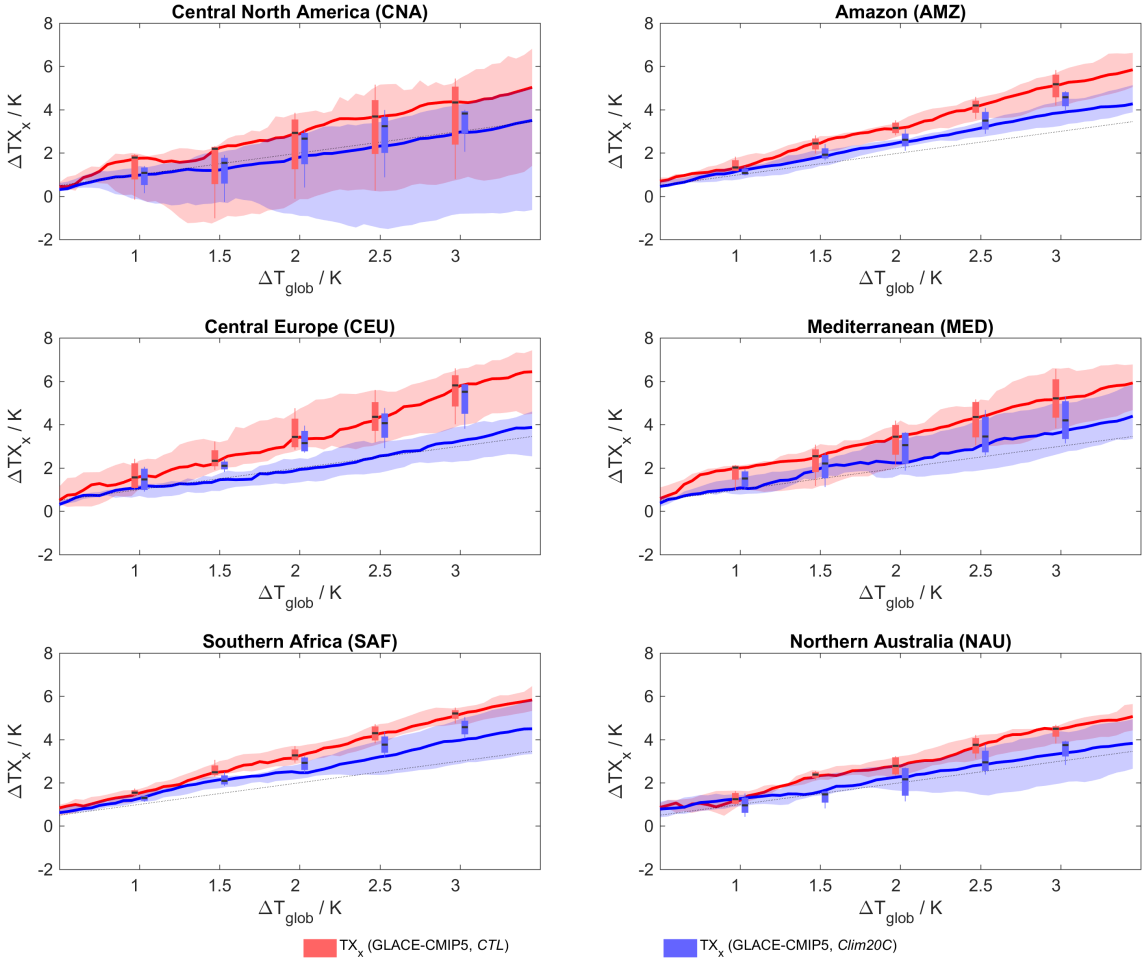

Figure 6. Changes of the yearly maximum value of daily maximum temperature $\Delta\mathrm{TX}_x$ scaled with global mean temperature increase ΔT_{glob} in the GLACE-CMIP5 experiments *CTL* (red color) and *Clim20C* (blue color) for six different SREX regions. $\Delta\mathrm{TX}_x$ and ΔT_{glob} both refer to the base period 1951–1970 (corrected with 0.22 K for the T_{glob} increase between 1871–1890 and 1951–1970). The shaded areas represent directly estimated $\Delta\mathrm{TX}_x$ from the GLACE-CMIP5 experiments *CTL* and *Clim20C*. The range of the shaded areas indicates the minimum and maximum values of all models, the line indicates the median. The red box-and-whisker plots are 20-year averages of $\Delta\mathrm{TX}_x$ in *CTL* (centered on the year when ΔT_{glob} reaches 1.0 K, 1.5 K, 2.0 K, 2.5 K, and 3.0 K). The blue box-and-whisker plots show the 20-year average $\Delta\mathrm{TX}_x$ minus the sensitivity-based soil moisture effect on $\Delta\mathrm{TX}_x$ (i.e., accounting for soil moisture effects on TX_x). The line in the box represents the median, the box the interquartile range, and the whiskers minimum and maximum values. The dashed curve indicates the identity line.

Earth Syst. Dynam. Discuss., https://doi.org/10.5194/esd-2018-34
Manuscript under review for journal Earth Syst. Dynam.
Discussion started: 7 June 2018

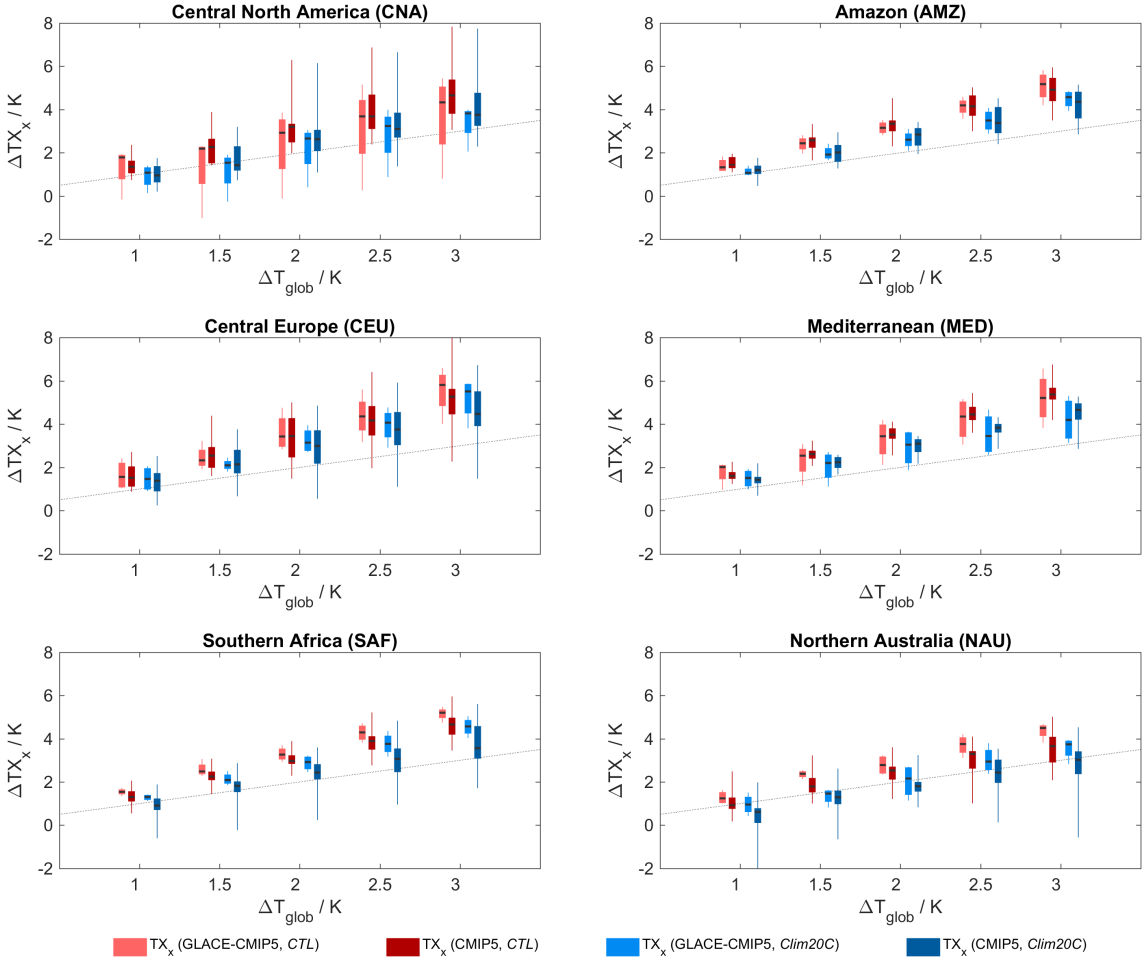

Figure 7. As in Figure 6 but including CMIP5 models and without directly estimated ΔTX_x from the GLACE-CMIP5 experiments. The different box-and-whisker plot groups (always containing four box-and-whisker plots) show the effects when ΔT_{glob} reaches 1.0 K, 1.5 K, 2.0 K, 2.5 K, and 3.0 K.